ResearchGate

See discussions, stats, and author profiles for this publication at: https://www.researchgate.net/publication/210112590

Silicon Nanocrystals Produced by Nanosecond Laser Ablation in an Organic Liquid

ARTICLE · FEBRUARY 2011

CITATIONS
8

READS
41

9 AUTHORS, INCLUDING:

Kamal Abderrafi
University of Valencia
19 PUBLICATIONS **162** CITATIONS
SEE PROFILE

Isaac Suarez
University of Valencia
58 PUBLICATIONS **258** CITATIONS
SEE PROFILE

Rafael Abargues López
Intenanomat S.L.
74 PUBLICATIONS **418** CITATIONS
SEE PROFILE

Available from: Rafael Abargues López
Retrieved on: 02 February 2016

THE JOURNAL OF PHYSICAL CHEMISTRY C

ARTICLE

pubs.acs.org/JPCC

Silicon Nanocrystals Produced by Nanosecond Laser Ablation in an Organic Liquid

Kamal Abderrafi,[†] Raúl García Calzada,[†] Maxim B. Gongalsky,[‡] Isaac Suárez,[†] Rafael Abarques,[†] Vladimir S. Chirvony,[†,*] Victor Yu. Timoshenko,[‡] Rafael Ibáñez,[†] and Juan P. Martínez-Pastor[†]

[†]UMDO - Unidad Asociada a CSIC-IMM, Instituto de Ciencia de los Materiales, Universidad de Valencia, P.O. Box 22085, 46071 Valencia, Spain

[‡]Department of Physics, Lomonosov Moscow State University, Leninskie Gory 1, 119992 Moscow, Russia

ABSTRACT: Small (3−5 nm in diameter following HRTEM images) Si nanocrystals were produced in a two-stage process including (1) nanosecond laser ablation of a Si target in an organic liquid (chloroform) that results in formation of big composite polycrystalline particles (about 20−100 nm average diameter) and (2) ultrasonic post-treatment of Si nanoparticles in the presence of HF. The post-treatment is responsible for disintegration of the composite Si particles, release of small individual nanocrystals, and reduction of their size due to HF-induced etching of Si oxide. The downshift and broadening of the ∼520 cm^{-1} Raman phonon band of the small Si nanocrystals with respect to the bulk Si Raman band is consistent with the presence of ∼4.5 nm Si nanocrystals. The photoluminescence spectra (450−900 nm) and decay kinetics of small Si nanocrystals were detected, and the possible origin of the luminescence is discussed.

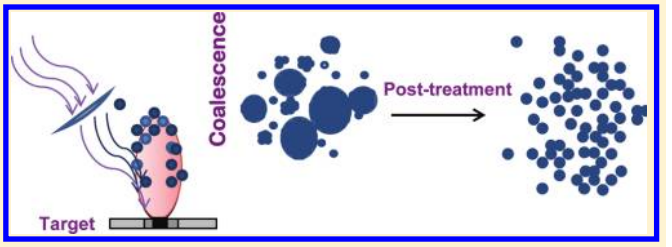

1. INTRODUCTION

Silicon nanocrystals (NCs) are a promising new material. A broad interest in this system is stimulated by its potential applications in light sources,[1] nonvolatile memory devices,[2] solar cells,[3] medicine (Photodynamic Therapy),[4] and bioimaging.[5] The most considerable obstacle on the way to a wide use of Si NCs in different applications is the lack of simple and inexpensive methods of their production. Besides, strict requirements are imposed for the nanoparticles used in living systems: first of all, the chemical purity of the product is important, a requirement which is difficult fulfill when the most commonly used chemical (wet) methods of synthesis are applied. Laser ablation in liquids (first of all in deionized water) is considered in the literature as a contamination-free green synthesis method[6] which meets, in general, all the above requirements.

An application of the method of a laser ablation in liquids (LAL) for production of Si NCs is still in its infancy. As a rule, Si NCs produced by this method are reported to be rather big (tens of nanometers and more) and possessing wide size distribution,[7] whereas most interesting for applications are nanoparticles, which exhibit quantum-confinement effect; in the case of Si NCs it corresponds to a diameter of the order of 5 nm and less. Only very recently Si NCs with an average size of several nanometers have been obtained by the LAL method.[8,9] In ref 8 very small Si NCs of the average diameter of 2.5 nm were produced in water by femtosecond laser ablation (120 fs pulses at 800 nm wavelength) at very low, near-threshold fluences of excitation light (0.05 J cm^{-2}). In ref 9 small-size Si NCs (average diameters of 3−7 nm) were produced by means of nanosecond laser ablation in ethanol, whereas much bigger particles were synthesized in water.[9]

Therefore, an important role of a liquid in LAL experiments directed to produce small-size Si NCs was discovered in ref 9, but details of this effect are not yet clear. The aim of the present work is to investigate the possibility of manufacturing small-size Si NCs by means of nanosecond laser ablation in organic liquids. We used chloroform, $CHCl_3$, as a medium to produce Si NCs by the LAL method because there is evidence in the literature about interactions of halogen-substituted hydrocarbons with Si nanostructures.[10] One can suggest that this interaction can be helpful for Si NC size limitation during the NC growth process similarly to the case of Au nanoparticle (NP) size limitations induced by the presence of organic molecules in water during laser ablation.[11]

2. EXPERIMENTAL DETAILS

A *p*-type Cz-silicon wafer of (100) plane with a resistivity of 10−20 Ω cm was ultrasonically rinsed first with deionized water and then ethanol for 1 h. The cleaned silicon wafer was used as a target, immersed in liquid medium ($CHCl_3$, or chloroform, 20 mL in an open glass vessel) and irradiated with the third

Special Issue: Laser Ablation and Nanoparticle Generation in Liquids

Received: September 30, 2010
Revised: January 17, 2011
Published: February 14, 2011

ACS Publications © 2011 American Chemical Society

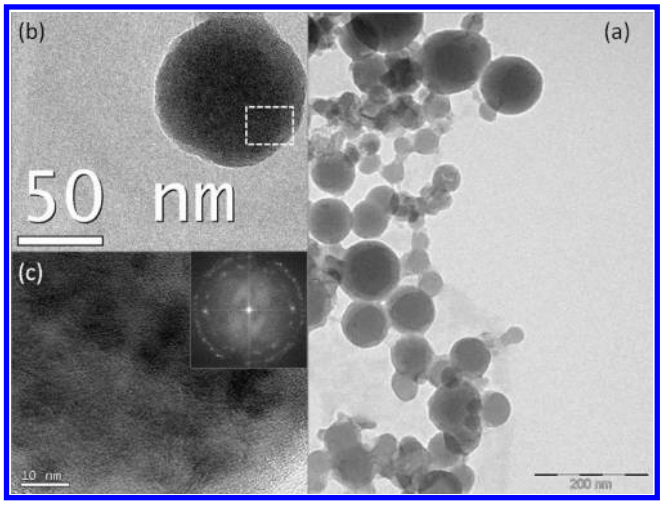

Figure 1. (a) TEM micrograph of silicon nanoparticles produced by laser ablation in chloroform. (b) HRTEM image of one big nanoparticle. (c) Amplified HRTEM image of the rectangular area outlined in (b). X-ray diffraction pattern is shown in the inset.

harmonic of pulsed Nd:YAG laser (355 nm, 40 ns pulse duration, 5 kHz repetition rate). The laser beam was focused by a lens having a focal length of 60 mm on the silicon target surface with a spot of about 30 μm diameter giving power densities per pulse ~40 J cm^{-2}. The solution was continuously stirred during laser irradiation. The target was scanned by the beam over the area of 56 mm^2 by means of an electro-optical beam deflector. A twenty-time repetition of the surface full scanning was found to be sufficient to observe the appearance of brownish color of the liquid, but usually hundreds of repetitions were applied.

After finishing the laser ablation procedure, an appropriate physicochemical post-treatment was applied as a second stage to obtain small-size monocrystalline silicon nanoparticles (NPs). First, chloroform suspension was transferred to plastic vessel. Then chloroform was evaporated under vacuum, and the precipitate formed on the vessel bottom was covered by the mixture of isopropanol, HF, and hexane (3:1:3). The vessel with the suspension was immersed in an ultrasound bath. Ultrasonic homogenizer "Sonoplus" HD 2200 (Bandelin) was applied for 30 min (power 80 W) for ultrasonic treatment of suspensions of Si NPs. All liquids used ($CHCl_3$, isopropanol, HF, hexane) were from Aldrich.

Si NPs obtained after the first (laser ablation) and second (post-treatment) stages were examined by transmission electron microscopy (TEM) with a JEOL-1200EX microscope and by High Rresolution TEM (HRTEM) with a FEI-TECNAI G2 instrument which were operated, respectively, at 100 and 200 KV. A suspension of Si NPs was placed on a copper mesh TEM grid coated on one side with carbon, and a solvent was completely evaporated at room temperature before transferring a grid with NPs into the microscope. NP size distributions were acquired by counting more than 500 NPs.

Raman scattering measurements were carried out under excitation with a 488 nm Ar-ion laser line using a Lab RAM HR800 micro-Raman system. Laser power was 100 mW, with accumulation time −3 scans of 60 s, and a 10× objective was used. Si NPs were deposited on the stainless steel surface by dropping a suspension and evacuation of a solvent by heating at 60 °C. This procedure was repeated about 10 times to increase

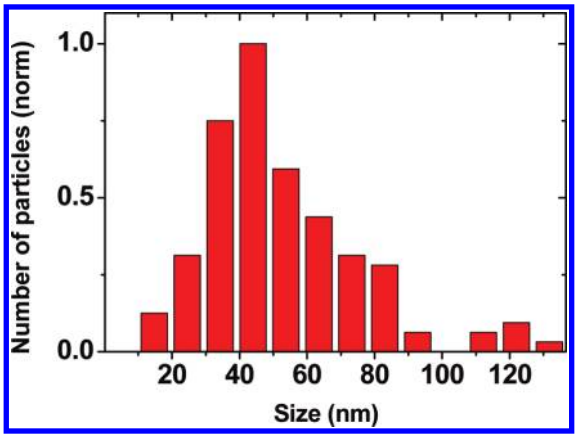

Figure 2. Size distribution calculated from TEM images of Si nanoparticles obtained by nanosecond laser ablation in chloroform.

the final concentration of Si NPs. All spectral experiments were done at room temperature in air.

The photoluminescence (PL) and PL kinetics were measured under excitation with a N_2-laser (wavelength λ = 337 nm, pulse duration τ = 10 ns, pulse energy E = 1 μJ, repetition rate ν = 100 Hz). The laser beam was focused by using a 20 cm lens into a spot of about 1 mm in diameter onto the sample (Si NPs on a quartz plate deposited by suspension dropping method). PL emission was collected on a 50 cm spectrometer equipped with a Si photomultiplier (time resolution of 100 ns).

3. RESULTS AND DISCUSSION

Laser ablation of a silicon target immersed in chloroform produced Si nanoparticles of a rather big size (tens of nanometers, see Figure 1). Particles are spherical in shape (Figure 1a and b), and their average size is about 50 nm. The size distribution of particles is shown in Figure 2. It should be noted that small particles with sizes less than 10−20 nm are practically absent in this distribution. HRTEM analysis of the morphology of these large-size particles shows that they have a polycrystalline microstructure. It was difficult to determine size distribution of the elementary crystallites inside the spherical particles shown in Figure 1a, but HRTEM images show the presence of monocrystallites with size of about 10 nm (Figure 1c; the corresponding XRD pattern is also shown as an inset).

We suggested that these polycrystalline Si NPs may consist of at least two materials: small Si crystallites visible in HRTEM images and Si oxide produced due to the presence of dissolved molecular oxygen in a liquid. We hypothesized that these complex structures can be disintegrated with simultaneous release of monocrystalline Si nanoparticles in the case when ultrasonic impact (for disconnection of the constituents) will be applied together with chemical treatment by HF (for silicon oxide etching).

The post-treatment procedure was implemented as follows. A transparent brownish suspension of silicon nanoparticles in chloroform was transferred into a plastic vessel. Then chloroform was evaporated, and the vessel was filled with a mixture of solvents isopropanol/HF/hexane (3:1:3). After shaking for a few seconds, the liquid mixture split into two parts: (1) a bottom (polar) part, consisting of isopropanol, water (as a part of HF solution), and HF, and (2) an upper (nonpolar) part, consisting of hexane.

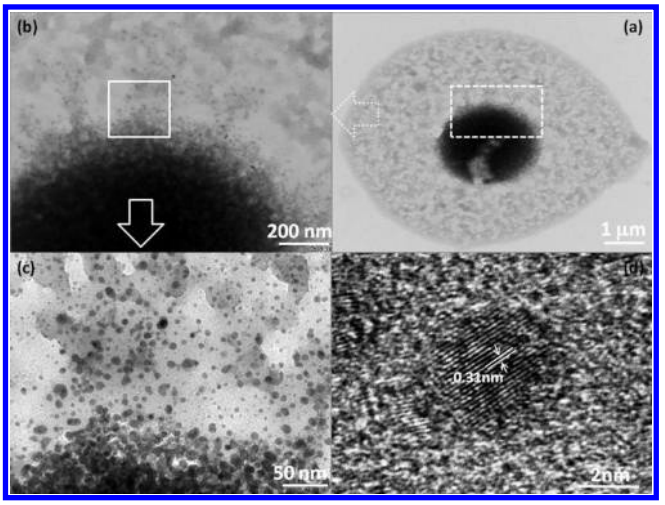

Figure 3. TEM micrographs of Si NCs after combined ultrasonic and chemical (HF) treatment: general view of NC agglomeration formed on the carbon membrane of the TEM grid (a and b); a view of individual NCs on the periphery of the agglomeration (c); and HRTEM of an individual Si NC (d).

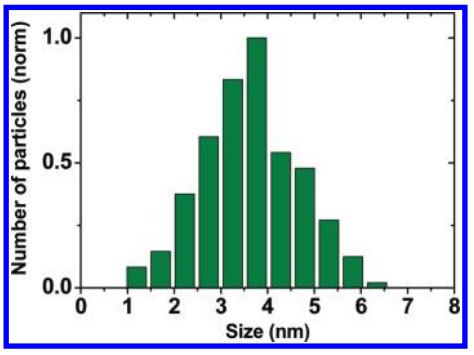

Figure 4. Size distribution calculated from TEM images of Si nanoparticles obtained by laser ablation in chloroform and then subjected to ultrasonic/HF post-treatment.

Before the beginning of the ultrasonic treatment all nanoparticles are in the bottom (polar) part of the liquid mixture. The location of nanoparticles in the bottom layer implies that their surface contains polar groups (usually Si−O and Si−OH formed due to Si surface interaction with molecular oxygen dissolved in liquids[12]).

Next, the suspension was subjected to ultrasonic treatment for 30 min. After the treatment, the bottom layer of the mixture became transparent, whereas the upper layer (hexane) acquired a yellowish color because all Si NPs turned out to be here. It implies that the Si NP surface became hydrophobic (due to surface covering by hydrogen[12]). Our preliminary FTIR measurements (in KBr tablets, not shown) performed with Si NPs extracted from hexane solution have also demonstrated the presence of a Si−H_x group characteristic band near 2100 cm^{-1}.

TEM micrographs of Si NCs after combined ultrasonic and chemical (HF) treatment are shown in Figure 3. For implementation of TEM measurements a drop of hexane suspension was deposited on the carbon membrane of the TEM grid. Evaporation of the solvent (hexane) led to the formation of a large agglomerate of nanoparticles with a total size of about 1 μm (Figure 3a, b). One can see in Figure 3c the presence of single

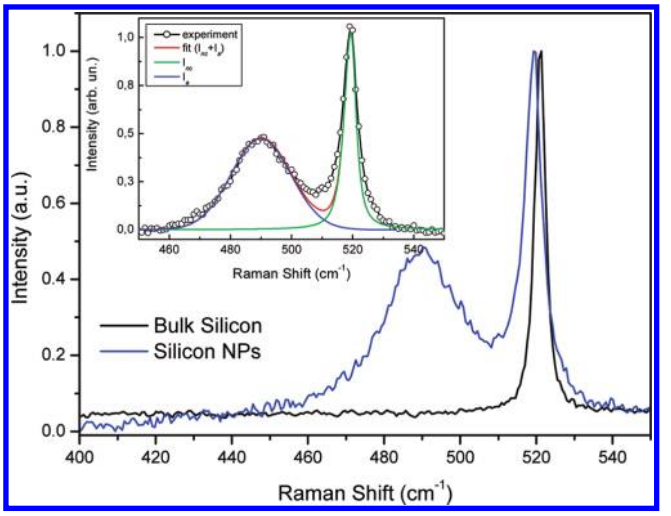

Figure 5. Raman spectrum of Si NCs after post-treatment (blue) as compared to the spectrum of bulk silicon (black). In the inset the same experimental Raman spectrum is shown (open circles) along with the model spectrum (red) obtained by summation of the model Gaussian (blue, for wide band at ~490 cm^{-1}) and modified Lorentzian (green, for narrow band at ~520 cm^{-1}) contours.

nanoparticles and their small clusters (consisting of a few particles) on the periphery of the agglomeration. Individual Si NPs (Figure 3d) exhibit a lattice fringe image spacing of 0.31 nm, which coincides with the (111) lattice constant for the Si diamond structure. Figure 4 shows typical size distribution of individual nanoparticles obtained by laser ablation in chloroform followed by ultrasonic post-treatment in the presence of HF. The maximum of this distribution is around 4 nm.

Raman spectroscopy provides information important for understanding the microstructure of Si NPs. Figure 5 shows Raman spectra of Si NPs after post-treatment (blue) and of bulk silicon (black). It is well-known that the bulk Si crystal displays a narrow optical phonon band at ~520.5 cm^{-1}. When Si crystallites become small enough (≤10 nm), the Raman phonon band broadens and shifts down in energy, and the shift can be connected with the crystallite size in the quantitative phonon confinement model by eq 1[13]

$$\Delta\nu = -52.3(0.543/D)^{1.586} \quad (1)$$

when $\Delta\nu$ is the shift (due to spatial confinement) of the Raman peak position of Si nanocrystals compared with the bulk value, and D is Si nanocrystal size ($\Delta\nu$ and D are in cm^{-1} and nm, respectively).

Namely, such a broadened and downshifted (2.0 cm^{-1} as compared to bulk Si) Raman band is observed for Si NPs produced in chloroform and then subjected to ultrasonic/HF post-treatment (Figure 5). Following (1), such a shift corresponds to 4.3 nm size of Si nanocrystals that is in good agreement with TEM-based size distribution.

Besides the band near 520 cm^{-1}, a broad band centered at 490 cm^{-1} is also detected for Si NPs produced by laser ablation in chloroform and subjected to post-treatment (Figure 5). It is known from the literature that this lower-energy Raman band belongs to disordered (amorphous) Si structures.[14] As one can see in the inset of Figure 5, the experimental two-band Raman spectrum (open circles) can be satisfactorily fitted by a sum of the modified Lorentzian (for narrow band at 520 cm^{-1}) and

dx.doi.org/10.1021/jp109400v |J. Phys. Chem. C 2011, 115, 5147–5151

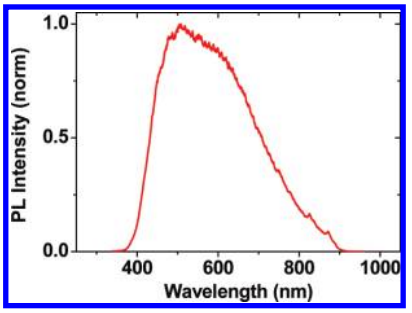

Figure 6. PL spectrum of isopropanol suspension of Si NPs produced by nanosecond LA in chloroform.

Gaussian (for wide band at 490 cm^{-1}). The origin of this amorphous silicon and its relation to Si nanocrystals is not yet understood. One of the possible explanations is that the amorphous Si can form a noncrystalline shell around the Si crystalline core, as has been found for Si NPs produced by LA in an inert gas atmosphere.[15] Indeed, some of our HRTEM images can be interpreted in favor of the presence of some amorphous layer around a crystalline core, but in most cases a distinct borderline of individual crystalline Si NPs is observed. Thus, we preliminarily suggest that the observed amorphous phase of silicon is likely produced independently and my be placed separately from Si NCs.

Luminescence properties of the obtained Si NPs have been also studied. It should be noted that, immediately after ultrasonic/HF post-treatment, Si NPs in hexane suspension do not show any remarkable PL. However, photoluminescence appears if hexane (with HF trace) is replaced by any liquid (in which dissolved oxygen of air is present) or hexane solution is deposited on subtract and kept on air. In both cases the PL is observed in the visible−near IR region, and its spectrum is shown in Figure 6 for the case of isopropanol suspension. The spectrum is rather broad (from ∼400 up to 900 nm) with a maximum near 500 nm.

In addition to Si NP luminescence spectra, the luminescence decay kinetics have been also measured. PL spectra of different Si structures can be rather similar, so that Si nanocrystals, Si−O related surface states, oxygenated amorphous Si, and oxygen defects in Si dioxide can exhibit PL spectra in the same spectral region. PL decay kinetics can give additional information and shed further light on the nature of the emitting states,[16] at least to distinguish between optically forbidden and optically allowed transitions.

Decay kinetics of the PL presented in Figure 6 was measured for wavelengths of 600, 675, and 750 nm. Representative PL decay kinetics obtained for 750 nm is shown in Figure 7. We applied the three-exponential decay model (red line in Figure 7)

$$I_{PL}(t) = A_1 \exp(-t/\tau_1) + A_2 \exp(-t/\tau_2) + A_3 \exp(-t/\tau_3) \quad (2)$$

(τ_i and A_i are decay lifetimes and their relative amplitudes) for fitting experimental decay kinetics (black line). For the kinetics measured at 750 nm, the following lifetimes and their amplitudes were obtained: $\tau_1 = 0.1\ \mu s$ ($A_1 = 0.78$), $\tau_2 = 7.8\ \mu s$ ($A_2 = 0.06$), $\tau_3 = 63\ \mu s$ ($A_3 = 0.16$). It was found that with detection wavelength decrease the decay profile remains approximately the same, but the short-lived signal becomes more prevalent, so that for $\lambda = 675$ nm, lifetimes (relative amplitudes) were found to be $\tau_1 = 0.08\ \mu s$ ($A_1 = 0.87$), $\tau_2 = 6.3\ \mu s$ ($A_2 = 0.05$), and $\tau_3 = 34\ \mu s$ ($A_3 = 0.08$)

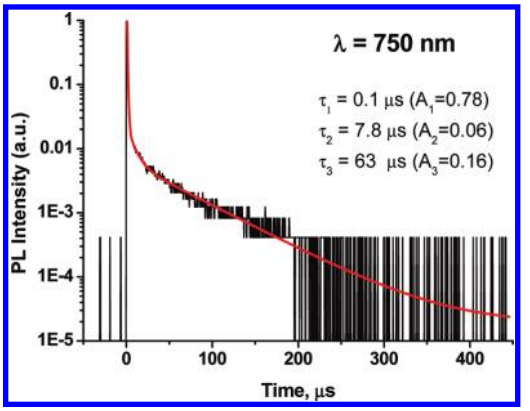

Figure 7. PL decay kinetics (λ_{reg} = 750 nm) of Si NPs produced by nanosecond LA in chloroform (after post-treatment).

and for $\lambda = 600$ nm $\tau_1 = 0.1\ \mu s$ ($A_1 = 0.95$) and $\tau_2 = 14\ \mu s$ ($A_2 = 0.05$), $A_3 = 0$.

Thus, as shown in Figure 6, the luminescence spectrum is heterogeneous and includes the emission of at least two centers with different lifetimes. Preliminarily, we suggest that emission centers with long-lived luminescence (lifetimes of tens of microseconds) may belong to the excitonic luminescence of silicon nanocrystals passivated by oxygen: in this case, yellow-red PL is usually observed possessing submillisecond lifetimes.[17] As for the nature of the luminescence with a short lifetime (less than 100 ns, time resolution of the setup), we found that relative intensity of the short-lived PL grows with time on the time scale of hours and days as a result of interaction with air that suggests the Si-oxide origin of this PL, the more so as Si−O related PL is usually short lived (nanosecond time scale).[18]

These assumptions about the origin of the two components of luminescence are in agreement with the behavior of Si NP PL in the presence of hydrofluoric acid. Indeed, HF removes silicon oxides that should result in quenching the short-lived photoluminescence. On the other hand, replacement of the oxygen passivation of silicon nanocrystals which emit long-lived PL on hydrogen passivation in the presence of HF should significantly change the PL properties. Indeed, unlike Si NPs passivated by oxygen, hydrogen-passivated silicon nanocrystals exhibit PL with nanosecond lifetimes, and this PL is usually observed in a different (blue-green) region.[19,20] In any case, the long-lived luminescence component belonging to oxygen-passivated Si NPs should be quenched in the presence of HF.

On the other hand, it is known from the literature that Si NCs passivated by chlorine show luminescence in the 1.8−3.1 eV spectral region,[21] which agrees well with the region of the emission of our Si NPs (in our case chlorine atoms can be released from chloroform during the laser ablation). Therefore, the origin of the observed PL and its relation to the Si NC surface require further investigation.

4. CONCLUSIONS

Thus, the results obtained by the methods of TEM, HRTEM, and Raman light scattering indicate that small (3−5 nm in diameter) Si nanocrystals are produced in a two-stage process including (1) nanosecond laser ablation of the Si target in an organic liquid (chloroform) that results in formation of big composite polycrystalline particles (about 20−100 nm average diameter) and (2) ultrasonic post-treatment of Si NPs in the

presence of HF. The post-treatment is responsible for disintegration of the composite Si particles, release of small individual nanocrystals, and likely, reduction of their size due to HF-induced etching of the Si oxide surface.

AUTHOR INFORMATION

Corresponding Author

*E-mail: vladimir.chyrvony@uv.es. Phone: (+34) 96 354 4050. Fax: (+34) 96 354 3633.

ACKNOWLEDGMENT

This work was supported through the Spanish MCINN and Generalitat Valenciana projects Grant Nos. TEC-2008-06756-C03-03 and PROMETEO/2009/074. The Raman spectra were measured by using equipment of the Center of User's Facilities of Lomonosov Moscow State University.

REFERENCES

(1) Walters, R. J.; Bourianoff, G. I.; Atwater, H. A. *Nat. Mater.* **2005**, *4*, 143.

(2) Tiwari, S.; Rana, F.; Hanafi, H.; Hartstein, A.; Crabbe, E. F.; Chan, K. *Appl. Phys. Lett.* **1996**, *68*, 1377.

(3) (a) Stupca, M.; Alsalhi, M.; Al Saud, T.; Almuhanna, A.; Nayfeh, M. H. *Appl. Phys. Lett.* **2007**, *91*, 063107. (b) Timmerman, D.; Izeddin, I.; Stallinga, P.; Yassievich, I. N.; Gregorkiewich, T. *Nat. Photonics* **2008**, *2*, 105.

(4) (a) Kovalev, D.; Gross, E.; Künzner, N.; Koch, F.; Timoshenko, V. Y.; Fujii, M. *Phys. Rev. Lett.* **2002**, *89*, 137401. (b) Chirvony, V.; Chyrvonaya, A.; Ovejero, J.; Matveeva, E.; Goller, B.; Kovalev, D.; Huygens, A.; de Witte, P. *Adv. Mater.* **2007**, *19*, 2967.

(5) (a) Park, J.-H.; Gu, L.; von Maltzahn, G.; Ruoslahti, E.; Bhatia, S. N.; Sailor, M. J. *Nat. Mater.* **2009**, *8*, 331. (b) He, Y.; Kang, Z.-H.; Li, Q.-S.; Tsang, C. H. A.; Fan, C.-H.; Lee, S.-T. *Angew. Chem., Int. Ed.* **2009**, *48*, 128.

(6) Kabashin, A. V.; Meunier, M. *J. Appl. Phys.* **2003**, *94*, 7941.

(7) (a) Dolgaev, S. I.; Simakin, A. V.; Voronov, V. V.; Shafeev, G. A.; Bozon-Verduraz, F. *Appl. Surf. Sci.* **2002**, *186*, 546. (b) Kazakevich, P. V.; Simakin, A. V.; Voronov, V. V.; Shafeev, G. A. *Appl. Surf. Sci.* **2006**, *252*, 4373. (c) Svrcek, V.; Sasaki, T.; Shimizu, Y.; Koshizaki, N. *Appl. Phys. Lett.* **2006**, *89*, 213113. (d) Du, X.-W-; Qin, W.-J.; Lu, Y.-W.; Han, X.; Fu, Y.-S.; Hu, S.-L. *J. Appl. Phys.* **2007**, *102*, 013518. (e) Umezu, I.; Minami, H.; Senoo, H.; Sugimura, A. *J. Phys. Conf. Ser.* **2007**, *59*, 392. (f) Svrcek, V.; Sasaki, T.; Shimizu, Y.; Koshizaki, N. *J. Laser Micro/Nanoeng.* **2007**, *2*, 15. (g) Takada, N.; Sasaki, T.; Sasaki, K. *Appl. Phys. A: Mater. Sci. Process.* **2008**, *93*, 833. (h) Yang, S.; Cai, W.; Zeng, H.; Li, Z. *J. Appl. Phys.* **2008**, *104*, 023516. (i) Svrcek, V.; Sasaki, T.; Katoh, R.; Shimizu, Y.; Koshizaki, N. *Appl. Phys. B: Laser Opt.* **2009**, *94*, 133.

(8) Rioux, D.; Laferriere, M.; Douplik, A.; Shah, D.; Lilge, L.; Kabashin, A. V.; Meunier, M. M. *J. Biomed. Opt.* **2009**, *14*, 021010.

(9) Yang, S.; Cai, W.; Zhang, H.; Xu, X.; Zeng, H. *J. Phys. Chem. C* **2009**, *113*, 19091.

(10) Sun, X.-H.; Li, C.-P.; Wong, N.-B.; Lee, C.-S.; Lee, S.-T.; Teo, B.-K. *J. Am. Chem. Soc.* **2002**, *124*, 14856.

(11) (a) Kabashin, A. V.; Meunier, M.; Kingston, C; Luong, J. H. T. *J. Phys. Chem. B* **2003**, *107*, 4527. (b) Sylvestre, J.-P.; Poulin, S.; Kabashin, A. V.; Sacher, E.; Meunier, M.; Luong, J. H. T. *J. Phys. Chem. B* **2004**, *108*, 16864.

(12) Kobayashi, M.; Liu, S.-M.; Sato, S.; Yao, H.; Kimura, K. *Jpn. J. Appl. Phys.* **2006**, *45*, 6146.

(13) (a) Zi, J.; Zhang, K.; Xie, X. *Phys. Rev. B* **1997**, *55*, 9263. (b) Paillard, V.; Puech, P.; Laguna, M. A.; Carles, R.; Kohn, B.; Huisken, F. *J. Appl. Phys.* **1999**, *86*, 1921.

(14) Maley, N.; Beeman, D.; Lannin, J. S. *Phys. Rev. B* **1988**, *38*, 10611.

(15) Orii, T.; Hirasawa, M.; Seto, T. *Appl. Phys. Lett.* **2003**, *83*, 3395.

(16) Hybertsen, M. S. *Phys. Rev. Lett.* **1994**, *72*, 1514.

(17) Wilson, W.; Szajovsky, P.; Brus, L. *Science (Washington, D.C.)* **1993**, *262*, 1242.

(18) Min, K. S.; Shcheglov, K. V.; Yang, C. M.; Atwater, H. A.; Brongersma, M. L.; Polman, A. *Appl. Phys. Lett.* **1996**, *69*, 2033.

(19) Belomoin, G.; Rogozhina, E.; Therrien, J.; Braun, P. V.; Abuhassan, L.; Nayfeh, M. H.; Wagner, L.; Mitas, L. *Phys. Rev. B* **2002**, *65*, 193406.

(20) Wolkin, M. V.; Jorne, J.; Fauchet, P. M.; Allan, G.; Delerue, C. *Phys. Rev. Lett.* **1999**, *82*, 197.

(21) Santana, G; Monroy, B. M.; Ortiz, A.; Huerta, L.; Alonso, J. C.; Fandiño, J.; Aguilar-Hernandez, J.; Hoyos, E.; Cruz-Gandarilla, F.; Contreras-Puentes, G. *Appl. Phys. Lett.* **2006**, *88*, 041916.